Fluorescence Based Nano Oxygen Particle (FNOP) for Spatiometric Monitoring of Cell Physiological Conditions

Manohar Prasad Koduri[1,6], Venkanagouda S. goudar[2], Yu-Wei Shao[3], John A. Hunt [4,5], Judith Curran[6], and Fan Gang Tseng[1,2,3,7]**

[1]International Intercollegiate PhD Program, National Tsing Hua University, Taiwan ROC.

[2]Department of Engineering and System Science, Frontier Research Center on Fundamental and Applied Sciences of Matters, National Tsing Hua University, Taiwan ROC.

[3]Institute of Nano Engineering and Microsystems, National Tsing Hua University, Taiwan ROC

[4] School of Science and Technology, Nottingham Trent University, Nottingham NG11 8NS, UK.

[5] Institute of Ageing and Chronic Disease, William Henry Duncan Building, University of Liverpool, Liverpool L7 8TX, UK.

[6] Department of Mechanical, Materials and Aerospace, School of Engineering, University of Liverpool, Harrison Hughes Building, Liverpool, L69 3GH, UK.

[7]Research Center for Applied Sciences, Academia Sinica, Taipei, Taiwan ROC.

Abstract:

Closed-loop artificial pancreas systems have recently been proposed as a solution for treating stage I diabetes by reproducing the function of the pancreas. However, there are many unresolved issues associated with their development, including monitoring and controlling oxygen, immune responses and the optimization of glucose. All of which need to be monitored and controlled to produce an efficient and viable artificial organ, that can become integrated in the patient and maintain homeostasis. This research focused on monitoring oxygen concentration, specifically achieving this kinetically as the oxygen gradient in an artificial pancreas made of alginate spheres containing islet cells. Functional Nanoparticle (NP) for measuring the oxygen gradient in different hydrogel cellular environments using fluorescence-based (F) microscopy were developed and tested. By ester bond, a linker Pluronic F127 was conjugated with a carboxylic acid modified polystyrene Nanoparticle (510 nm). A hydrophilic/ hydrophobic interaction between the commercially available oxygen sensitive fluorophore with F127 results in Fluorescence-based Nano oxygen particle (FNOP). The in-house synthesized FNOP was calibrated inside electro sprayed alginate filled hydrogels and demonstrated a good broad Dynamic Range (2.73-22.23) mg/L as well as a Resolution of -0.01 mg/L with an accuracy of ± 4%. The calibrated FNOP was utilised for continuous measuring of oxygen concentration gradient for cell lines RIN-m5F / HeLa for more than five days in alginate hydrogel spheres *in vitro*.

Keywords: Bio Sensors, Fluorescence, HeLa Cells, Oxygen Sensor, Optical sensors, RIN-m5F

1. Introduction:

According to the world health organization, diabetes is one of the top fifteen leading causes of death in the world for the year 2002, though it is projected to be in 7th position by 2030 [1], but currently in 6th position and accounted for approximately 1.6 million deaths in 2015. There was approximately a 50% increase in death due to diabetes from 2000 to 2012. This disease still urgently requires medical therapies to tackle the fatalities and to deliver cost effective strategies for the detection and treatment of the disease. It is necessary to develop techniques which can detect, monitor and cure the disease. Currently there are a number of technologies which can help to tackle the effects of diabetes and the development of bio-artificial pancreas is one strategy with promise by providing insulin production and release [2].

To produce a bio artificial pancreas, Beta cells are encapsulated in biocompatible material, cultured *in vitro* and then injected into patients [3]. Theoretically the cells in the encapsulated material will respond accordingly to the glucose level [4]. A major limiting factor in the development of the artificial pancreas is the optimization of encapsulation. The encapsulation material must defend the cells within from the host immune response, allow the release of exogenous factors produced by the encapsulated cells, and provide for the necessary mass transport exchange of nutrients, oxygen and other factors that are essential to maintain the encapsulated cells [5, 6]. Therefore, the material must act as a selectively permeable barrier. The size and composition of the encapsulating material or hydrogel is also a critical factor in the performance of the artificial pancreas. In the work by Vegas, A. J et.al [7], the sizes of alginate spheres were varied in the range of 0.5mm to 1.5mm and it was observed that the 1.5mm modified alginate spheres were advantageous in terms of reducing immunological responses when compared to 0.5mm sized spheres. However, the oxygen distribution across the larger sphere varied with few cells remaining

inside the centre of the sphere [7]. In this research the oxygen distribution within spheres has been evaluated. Different concentrations of calcium and strontium gelated alginate spheres were utilised as the cell carrier and the hydrogel sizes were in the range 700-1000 μm in diameter.

Primary human derived donor cell encapsulations have proven efficacy in terms of diabetes control, there is a shortage of donor cells for socioeconomic reasons. To address this issue of a shortage of donor cells, some groups are encapsulating embryonic stem cells in hydrogels, and differentiating the cells [8]. The physiological balance of oxygen, pH, and glucose levels in and around the hydrogel are key parameters in controlling the differentiation [9]. In particular, oxygen concentration plays a key role in the initial survival of encapsulated cells [10-12]. Deriving information regarding levels of oxygen concentration inside the material in a high spatial and temporal distribution will permit the synthesis of new material systems where cell growth and performance can be enhanced [13]. Potentially real time monitoring of oxygen levels can be achieved by fluorescent technologies.

The first oxygen sensing mechanism by fluorescence was demonstrated by Kautsky in the early 20th century [14], the first fluorescence system with an integrated UV source was developed in 1968 by Bergman [15]. A wide variety of fluorophores [16] like organic probes, metal-ligand complexes, and luminescent nanomaterials make this technique versatile. Metal-ligand complexes have a longer lifetime, and large stoke shift and are more stable when compared to organic probes. In metal-ligand complexes, Ruthenium-based oxygen sensing is the most studied and widely used fluorophore because of its wideband excitation (400-480 nm) and large stoke shift, resulting in an emission region of >610 nm. The importance and working principle of the fluorescent responsive ruthenium dye were explained by Mills. A and M.P. Coogan et al [17, 18]. Based upon data derived from previous reports a hydrophobic fluorophore of the ruthenium-based metal-ligand complex

was selected for our sensing application. To avoid the photo-bleaching effect of the fluorophore, a suitable substrate material has to be chosen and this provided broad adaptability to the specific needs [19]. A fluorophore can be tethered or encapsulated onto a substrate material [20] and it can be in the form of a thin film or particle. Within this paper, data is presented which provides evidence that the particle-based approach can provide spatiometric concentration gradient information from inside an encapsulated material for 3D tissue culture applications. The advancement of nanomaterial technology and their application in biocompatibility has huge potential in optimizing the design and of substrate materials and controlled culture conditions to induce specific forms of cell responses. [21, 22]

Previous work has successfully demonstrated the encapsulation of fluorophores in a nanoparticle for intracellular imaging [23], but very few works utilized these sensors for material optimization, via monitoring of selected parameters within a hydrogel environment that provides real time information regarding optimal environmental conditions that are required to ensure efficient cell function [24]. Previous studies have utilized commercial sensors [25] which are not suitable for the new generation of additive manufacturing techniques due to their large feature size of sensors which may affect toxicity and biocompatibility for a wide range of cellular phenotypes [26]. To address these issues small feature Oxygen sensors, with easy calibration, and reduced photo bleaching must be designed and tested. The objective of this research was to fabricate nanoparticles that have the ability to sense a range of oxygen concentrations by binding optical responsive fluorophores on to them and employing these sensors in 3Dimensional cellular conditions.

2. Materials and Methods:

2.1 Materials and Reagents

Polystyrene Nano beads with surface modified by carboxyl groups (Thermo SCI-ENTIFIC, W050C), Pluronic F127, (3-Aminopropyl) triethoxysilane, Strontium chloride, Calcium chloride dehydrate, Alginic acid sodium salt (Sigma Aldrich), Ru (dpp) 3Cl2 (C72H48Cl2N6Ru) (Fluka) (excitation at 470-490 nm and emission at 613 nm), HeLa cell lines, RIN-mF5 cells lines, Culture well gaskets (Grace Bio Labs), Cell culture Media Gibco™ RPMI 1640 Medium 1x, Gibco™ DMEM 1x ,SPl life science culture flask, Hamilton syringe (25ul), KD scientific syringe pump, Nitrogen and Oxygen gas cylinders (10 L), Oxygen meter (Hanna Instruments 98193), KUBOTA centrifuge 3700, MIKRO 200R centrifuge, SPELL MAN voltage controller (9 W, 30 kV | CZE1000R), JEOL JSM 6610 SEM, Zeiss LSM 780 Confocal Microscope - Inverted Microscope were employed in this study.

2.2.1 Synthesis of Functional Nano Oxygen Particles

FNOPs were fabricated using the process in fig. 1A. 0.5ml (100mg/ml) Polystyrene Bead (PSB) solution was centrifuged at 8000 rpm for 10 minutes to extract the PSBs from the Sodium azide solution. To obtain pure PSBs a purification step was repeated in twice, DI water was mixed with PSBs and centrifuged at 8000 rpm for 10 minutes, and the supernatant was removed as well as the samples were mixed with DI water and centrifuged for a second time. The supernatant was removed and DI water was added to make a final solution of 1ml PSB solution. Pluronic F127 (0.1g/1ml of PSB) (a triblock copolymer), poly (propylene oxide) (a central hydrophobic polymer), and poly (ethylene glycol) (PEG, hydrophilic ends) were employed and attached to the surface of PSB by an esterification process, 1 mg of Oxygen-sensitive red fluorescent molecule Ru (dpp) 3Cl2, (C72H48Cl2N6Ru) (Fluka, excitation at 470-490 nm and emission at 613 nm), was attached to the structure of a hydrophobic polymer Pluronic F-127 [27]

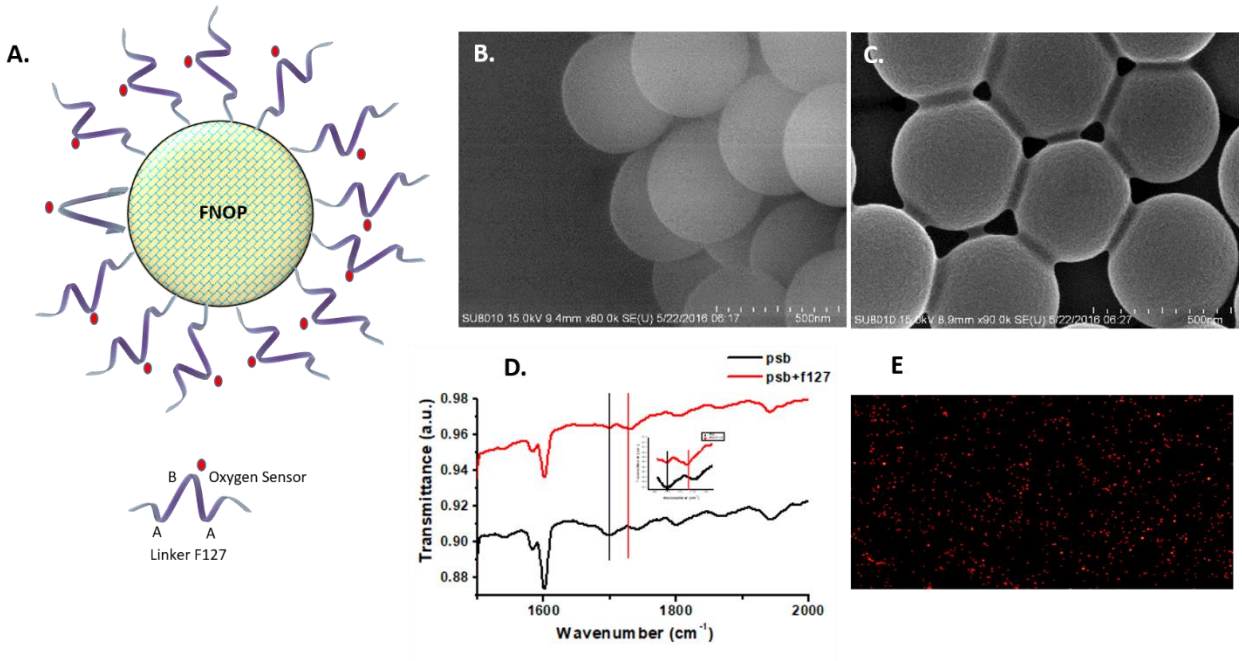

Figure 1. (A) Schematic illustration of FNOP (B) SEM image of PSBs after surface modified with carboxylic functional group. (C) SEM image of PSBs after F127 grafted. (D) Comparison of FTIR Transmission spectrum of B and C (E) Fluorescence image of FNOPs

in ethanol and ultra-sonicated for at least 30 minutes to form functional FNOPs by hydrophobic interaction. Functional FNOP particles were washed with sterile DI water by centrifuging the sample at 8000 rpm for 10 minutes, the supernatant was removed. Finally, 1ml of sterile DI water was added to the washed FNOP. The final Functional FNOPs were stored in a dark and dry place at room temperature for further experiments. To ensure spatiometric dispersion of particles throughout the suspension and to avoid aggregation because of electrostatic effects a centrifugation of FNOP stock solution at low speed of 1100 rpm for ten minutes was introduced prior to use in calibration and sensing experiments.

Nanoparticles were visualized using Scanning Electron Microscopy (Fig. 1 B and C). The corresponding FTIR image (Fig 1D), suggested that the room temperature esterification process for two hours was successful in attaching PSB particles with Pluronic F127 and corresponding

fluorescence image (Fig 1E) of functional Nano oxygen particles with excitation of 470 nm and emission >610 nm.

2.2.2 Hydrogel Preparation

2.2.2. A Preparation of alginate solution

A sterilized 5 wt. % alginate solution was prepared using Alginic acid mixed with DI water on a magnetic stirrer for 12 hours at 50^0C. The prepared solution was kept for sterilization in an autoclave and stored in 4^0C until required. The hydrogels 5wt. % alginate was mixed with filtered culture media to make a 3 wt. % solution.

2.2.2. B Electrospray technique

The hydrogel spheres were prepared using electrospray technique [28]. Sterilized alginate solution was loaded into a Hamilton syringe (25ul) (Fig 2A). The positive terminal of a high voltage power supply (5-7KV) (SPELL MAN voltage controller) was connected to the needle of the syringe and the ground terminal was applied to a metal container loaded with either Strontium chloride (0.1M SrCl2) or Calcium chloride (0.1M Calc2) for the polymerization of alginate (concentrations optimized based on data derived from experiments described in section 2.2.7). The polymerized alginate hydrogel spheres were collected and further used for calibration and validation experiments. The hydrogel spheres were imaged with a confocal microscope and the structure of half spheroid and the sensor distribution inside hydrogel (Fig. 2B) which was taken with the aid of confocal microscope with a total z-axis of 400 μm in step size of 6 μm.

Equipment was sterilized by spraying 70% ethanol and kept under UV irradiation for at least 2 hours before the experiment. For measuring the oxygen concentration within cellular environments, the 3 wt. % alginate was mixed with the RIN-m5F/ HeLa cell lines in a

concentration of 2.00×10^6 (cells/ ml) / 5.00×10^6 (cells/ ml) for further generation and testing of hydrogels.

A MOXI Z Mini Automated Cell Counter Kit, US Version was used in measuring cellular concentration. In 1ml final volume of PBS washed trypsinzed cell a 75ul of cell solution is loaded onto the cell counting cassette and corresponding cellular concentrations were noted.

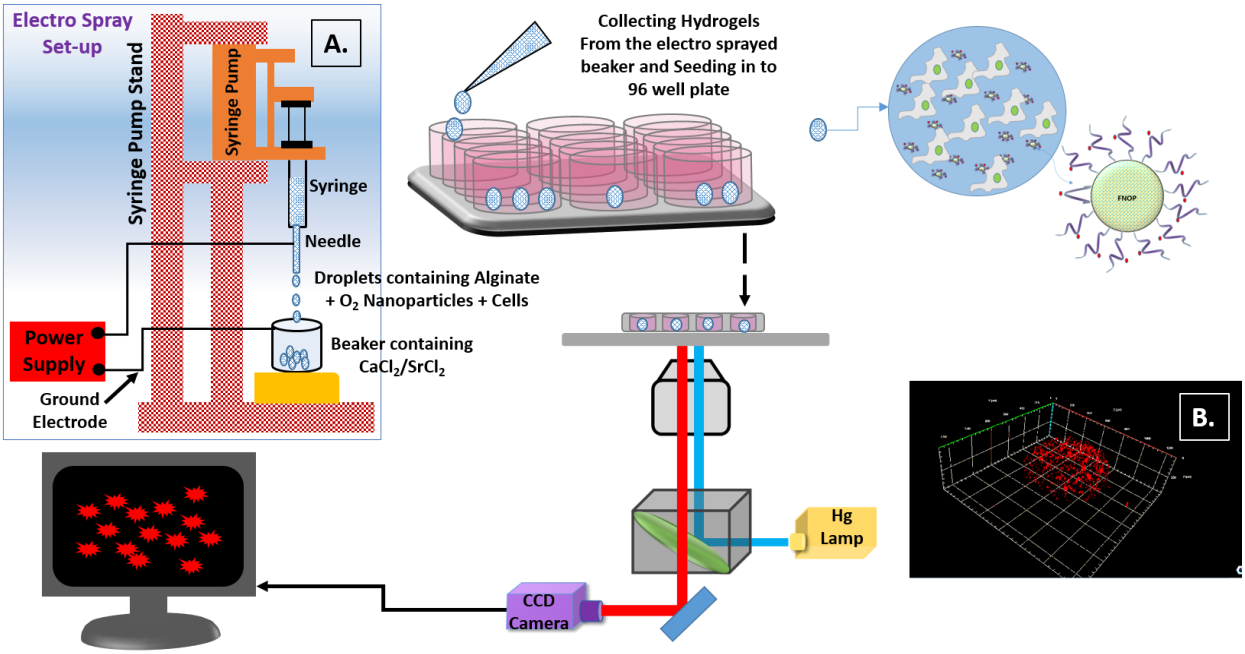

Figure (2A) Electrospray technique in generating hydrogels (2B). confocal imaging of generated hydrogels with FNOP sensor.

2.2.3 Calibration of oxygen

A glass container filled with DI water was used for calibration, as shown in fig. S1a. The containers contain 3 inlets for input of oxygen and nitrogen gases, as well as inserting the oxygen meter (Hanna Instruments 98193) which was used to monitor dissolved oxygen. One gas outlet was fitted with the rubber lid for free flow of gases into the chamber [29].

For calibration of oxygen in a hydrogel sphere, the alginate solution was mixed with 10 to 20ul of FNOPs and stirred for 5 minutes using a magnetic stirrer and then the hydrogels of size ~750

μm were generated by using the technique as specified in section 2.2.2.B. The generated hydrogels were collected and pipetted evenly on to the well gasket filled with alginate. The glass slide with alginate hydrogels was placed in the water-filled container and monitored under the microscope.

For calibration in DI water, the FNOP particles were pipetted onto a modified glass substrate with the 3-Aminopropyltrimethoxy silane treated and attachment of PSBs were done by attachment of leftover carboxylic acid group on PSB to the amine functional group forming the amide bond.

2.2.4 Cell Culture

All cultures were maintained in 5% CO2, 95% air, and at 37^0C

2.2.4. A HeLa cell lines

HeLa cell lines, were purchased from Bio resource Collection and Research Center (BCRC) and grown media consisting with Gibco™ DMEM 1x with 10% foetal bovine serum (FBS) (GIBCO), 1% penicillin – streptomycin (AppliChem).

2.2.4 B RIN-m5F cell culture

RIN-m5F cell lines, an islet beta cell, was purchased from Bio resource Collection and Research Center (BCRC) and grown media consisting with Gibco™ RPMI 1640 Medium 1x, 10% foetal bovine serum (FBS) (GIBCO), 1% L glutamine (200 mM Solution, GIBCO), 1% penicillin – streptomycin (AppliChem).

2.2.4 C Cell staining

2.2.4 C.A Hoechst

5ug/ml of Hoechst was dissolved in PBS solution and for each cell culture flask 2ml stain suspension was added and incubated for 30 minutes. The stained cell flasks were washed with PBS to remove unbounded Hoechst. Hoechst labelled cells were trypsinzed and resuspended into the

appropriate concentrations for incorporation into the hydrogel experiments. RIN-m5F stained with Hoechst (Fig.S2a).

2.2.4. C.B Calcein AM Viability Stain

In initial experiments, before the encapsulation of cells into hydrogels, cells were stained with Hoechst, Hoechst intensity could not accurately determine cell viability, as the intensity decreased with time (Fig.S3) and detection of the Hoechst signal is compromised by background staining and noise, (Fig.S4). To analyze cellular viability, Calcein AM was used at regular intervals, using a batch processing technique for cellular viability in RIN-mF5 cells in hydrogels. A 1ul of Calcein AM stock solution (1ug/1ul) was dissolved in 1ml of FBS free medium and 200 µlof the dissolved or working solution was taken and used in a batch process by adding into each well of a 96 well plate. Insulin cells stained with Calcein AM in 10 ml T75 flask (Fig.S2b).

2.2.5 Toxicity

The FNOP particles were characterized for toxicity, with a varied concentration range (10µl/ml to 50µl/ml in a step size of 10µl/ml) of Nanoparticles were cultured in contact with 1.14×10^5 Hela cells in 10 ml T25 flask for 8 days and obtained the optimized concentration of 10-20 µl of FNOPs as shown in Fig.S5.

2.2.6 Analysis

2.2.6 A. Image processing

The fluorescence intensities of the FNOPs were acquired by a camera through an optical microscope (OM) with the help of Cam-ware and analyzed by image software (Image J). The colour images were converted into 32 bit black and white images.

With the aid of Calcein AM staining, the cellular density inside the hydrogel was calculated. This was achieved by subtracting the background from the positive colour cellular images (positive

Calcein stain) and then converting the images to grayscale. Threshold levels were adjusted for images to separate the background pixel intensity form the foreground pixel intensity and the number of the particles with suitable pixel size (within the size of cells) were turned in to a binary image, measured and plotted.

2.2.6 B. Statistical Analysis

To measure the oxygen concentration, an average of 10 FNOP intensities were analyzed for every hydrogel image. To measure a cellular density, 3 hydrogels stained with Calcein AM were analysed and the average value was used as the reference value, and corresponding standard deviation values were plotted as error bars. For curve fitting processes in analyzing graphs, the origin was used.

2.2.7 Hydrogel as a scaffold

To evaluate the effect of different concentrations and type of gelling agents on cell viability a series of screening experiments were conducted. RIN-m5F cells (Fig.S6a) and HeLa cells (Fig.S6b) were cultured in contact with the five different hydrogel test conditions by seeding 1.0×106 cells per well in a 6 well plate, 3wt % alginate solution, 100mM Calcium chloride, 100mM strontium chloride solution and alginate (3wt %) solution was gelated with Calcium chloride and Strontium chloride to form a thick substrate. In optimizing the molar concentration of CaCl2 and SrCl2 a range (10mM to 450mM) with a step size of 50mM were tested and better gelation was observed at 100mM concentration, this was used for optimized electrospray generation of hydrogels.

In Fig. S6a, RIN-m5F cells were cultured for 7 days without any media change, this provided for the observation of cells under the control label (cells with media) were showing a feature of floating (from 60 hours) which is a characteristic nature of Insulin cell. Though the concentration

(100mM) of calcium chloride and strontium chloride was high, however after generating hydrogels, the hydrogels were washed for 3 times with the respective culture medium to ensure that leftover calcium or strontium ions should not affect the cells in hydrogels. The thin film approach of 3wt. % alginate solution cured with calcium and strontium ions (figure S6a) clearly shows good growth of cells. The calcium gelated alginate scaffold substrate demonstrated more effective growth of RIN-m5F cells when compared to strontium gelated alginate within a thin film structure (Fig. S6a). Though the control experiments showed some progressive results in the approach to optimizing the hydrogel-based approach for the RIN-m5F cell culture. The parameters obtained cannot be completely relied on from this approach to be applied further for the 3D spheroid model, because the structural and environmental conditions differed 2D model to 3D model.

2.2.8 SEM sample preparation

For imaging the FNOP sensors, the sensors were pipetted onto the Silicon wafer and then dried under room temperature, coated with chromium, for about 10 to 15 nm for visualization under SEM.

For imaging the hydrogels, alginate was pipetted onto the glass slide and then gelated with calcium and strontium ions. The gelated hydrogels were dried under room temperature and the dried sample was placed onto sample holder with the aid of carbon tape and coated with chromium for about 10 to 15 nm for visualization under SEM.

Results and Discussion:

The optimized FNOP/cell concentration was used to assess the effect of culturing FNOPs in contact with RIN-m5 cells and no toxic effect was observed. Results from this initial study also

demonstrated that FNOPs were able to enter inside or attach to the HeLa cells whereas no observable FNOP particles were inside the Insulin cells (Fig.S7a, b).

As specified in section 2.2.3 and 2.2.6 the calibration of oxygen was carried out inside the hydrogel (fig.3A, B, and C) and in DI water (fig.S1b). The calibrations inside hydrogels were performed at 17^0C which was different from the room temperature, this was due to purging nitrogen gas into the chamber which decreased the water temperature (measured with temperature sensor embedded in the oxygen meter). The oxygen concentration was varied and obtained a measurable range of (2.73-22.23) mg/L, Percentage of oxygen saturation was correlated to the dissolved oxygen (DO) in mg/L by multiplying a factor of 0.69 in measuring DO levels at 37^0C, which is approximated by using Winkler method. In DI water the synthesized FNOPs showed good approximation to the characteristic nature of stern Volmer relation [11]. In addition to the calibration, the FNOP particles were observed in the hydrogel environment for 7 days and the intensity of calibration was measured at regular interval (Fig. 3D). The hydrogels were maintained in the same culture environment as standard cell culture. The curve clearly showed that there was no significant deviation in the intensity of FNOPs. This suggests that there was negligible photo bleaching. To minimize the effect of saturation of pixel intensity, the camera exposure time was optimized to 1 sec exposure as it had the least photo bleaching effect when compared to 2, 3, 4 and 5 sec camera exposure time.

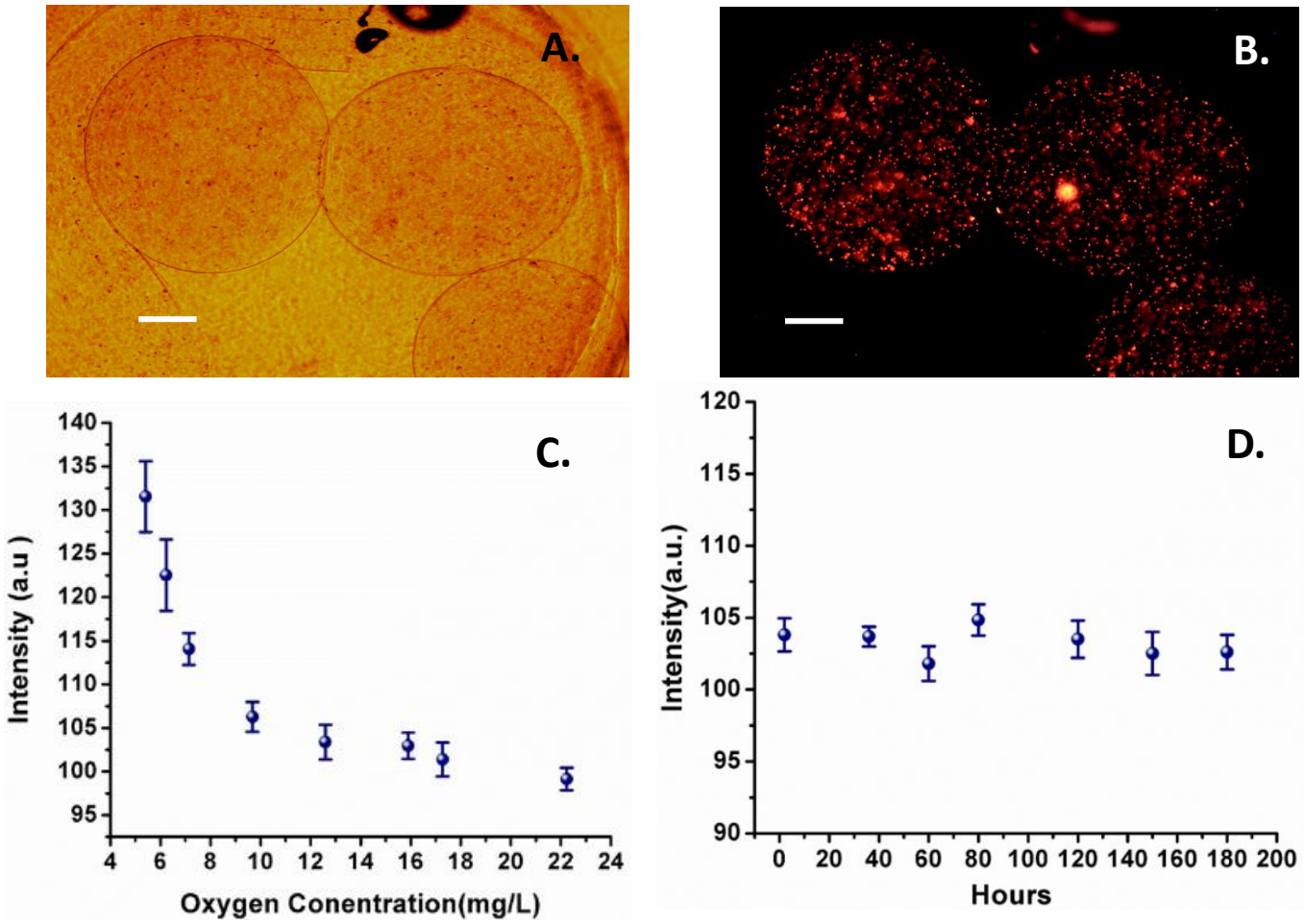

Figure (3A). Bright field view Hydrogel (3B). Fluorescence intensity of FB-FNOP at particular oxygen concentration (3C). Calibrated curve for different oxygen concentrations 3D. Intensity vs Number of hours for photo bleaching effect [Scale bar-200 μm]

Each hydrogel was generated with 700-800 RIN-m5F cells by considering 2.00×10^6 cells/ ml in alginate solution. The generated hydrogels were collected using pipette tips and were distributed evenly in the 96 well plate culture chamber, incubated at 37^0C, 5 % CO2 and were monitored. The fluorescent image for sensing oxygen and RIN-m5F cellular viability was taken at respective time intervals (fig. 4.A, B, and C).

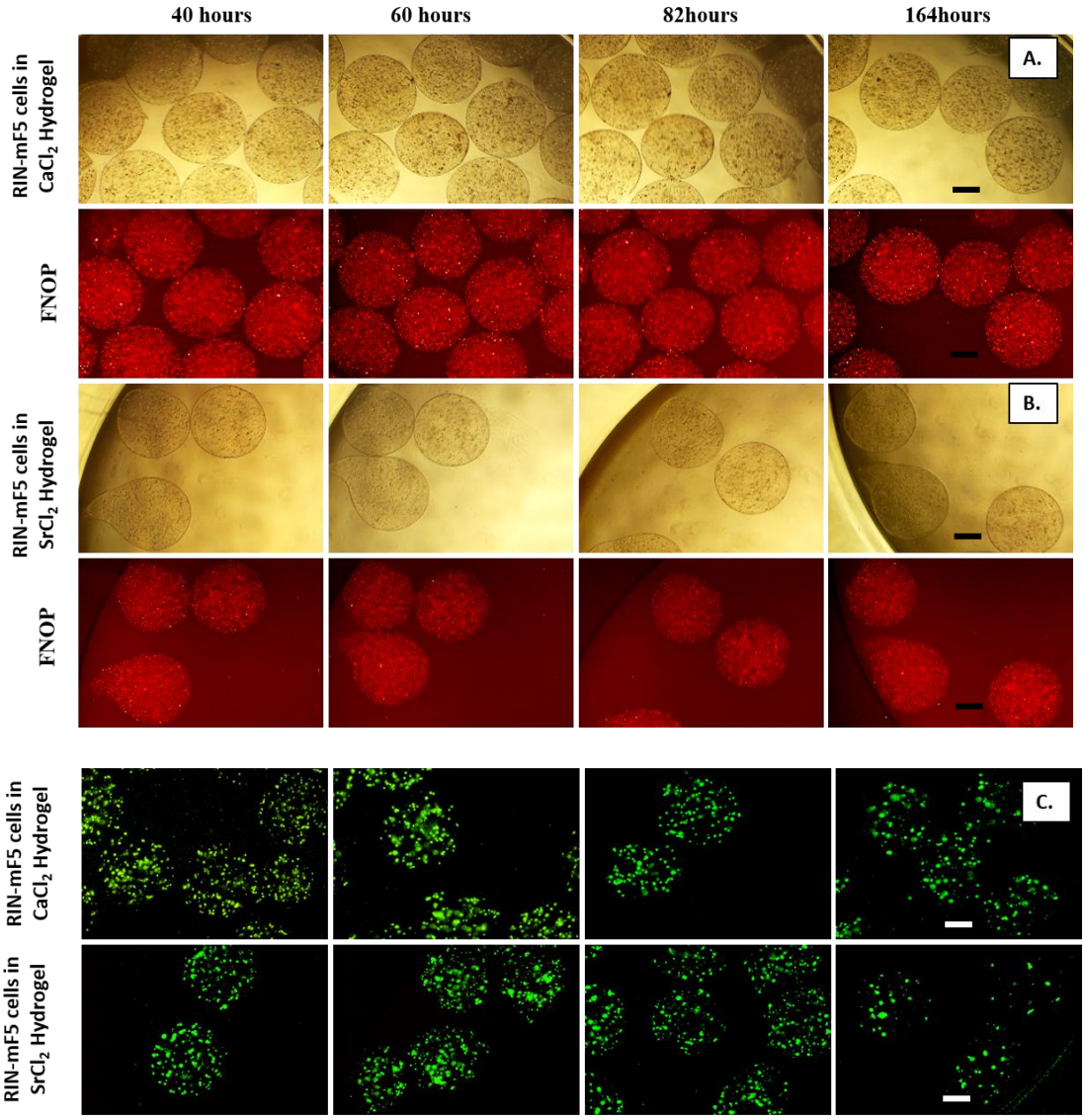

Figure (4A) Culturing of RIN-m5F in CaCl2 gelated Hydrogel Red colour indicated the FNOP (4B). Culturing of RIN-m5F in CaCl2 gelated Hydrogel Red colour indicated the FNOP (4C). CaCl2 (Top) and SrCl2 (bottom) gelated Hydrogel environment of RIN-m5F stained with Calcein AM. [Scale bar-350 µm]

The oxygen levels within hydrogel were measured by using a reference calibration (Fig. 5A). Oxygen gradients in both hydrogels showed the upward curvature and position of change can be correlated with respective time constants deduced from figure 5B, there was an exponential decay

in cellular density with time. By using a mathematical curve fitting technique, time constants for CaCl2 and SrCl2 hydrogels were approximately 120 and 45 hours respectively.

From the Fig.4C, 5A and 5B, it was observed that RIN-m5 cells were more viable in calcium-based hydrogels when compared to Strontium based hydrogels. Within the hydrogels, the exterior parts had greater viability compared to the interior parts or necrotic parts, this was due to the oxygen gradient in the CaCl2 hydrogel environment of RIN-m5 being nearly an inverse square to the radial distance.

For insulin cells, the normalized intensity levels, in a CaCl2 gelation hydrogel were divided into three regions (Centre, Interior, and Exterior), the corresponding intensity was plotted with time (Fig.6) Oxygen concentration was inversely proportional to intensity. By correlating the Initial normalized average intensity with Oxygen a difference of approximately 1.22 mg/L and 0.61 mg/L was observed with the exterior region and interior respectively with a centre region, and difference of 0.54 mg/L was observed between interior and exterior regions.

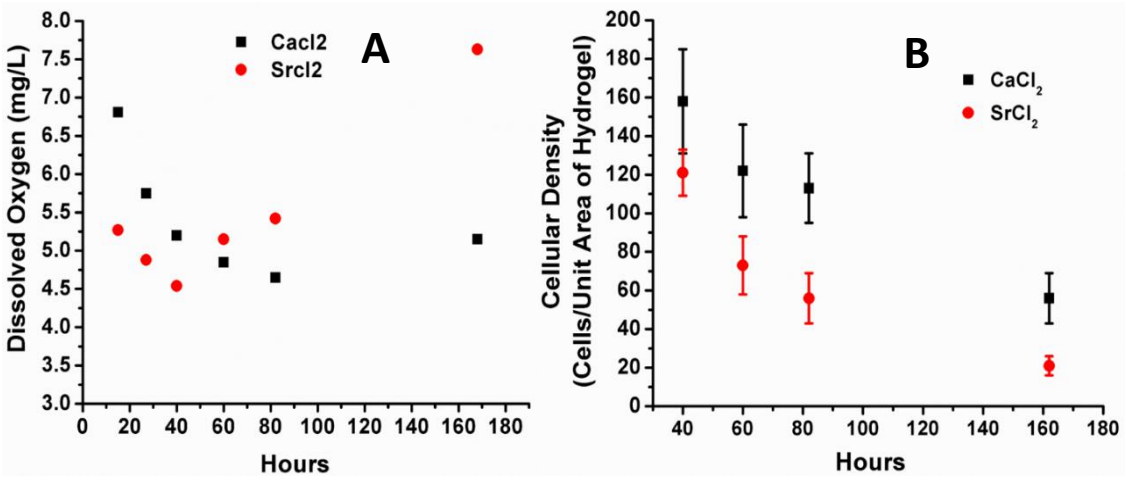

Figure (5A). Oxygen gradient in SrCl2 and CaCl2 gelated Hydrogel environment of RIN-m5F cells (5B) Cellular density of CaCl2 andSrCl2 gelated Hydrogel environment of RIN-m5F stained with Calcein AM

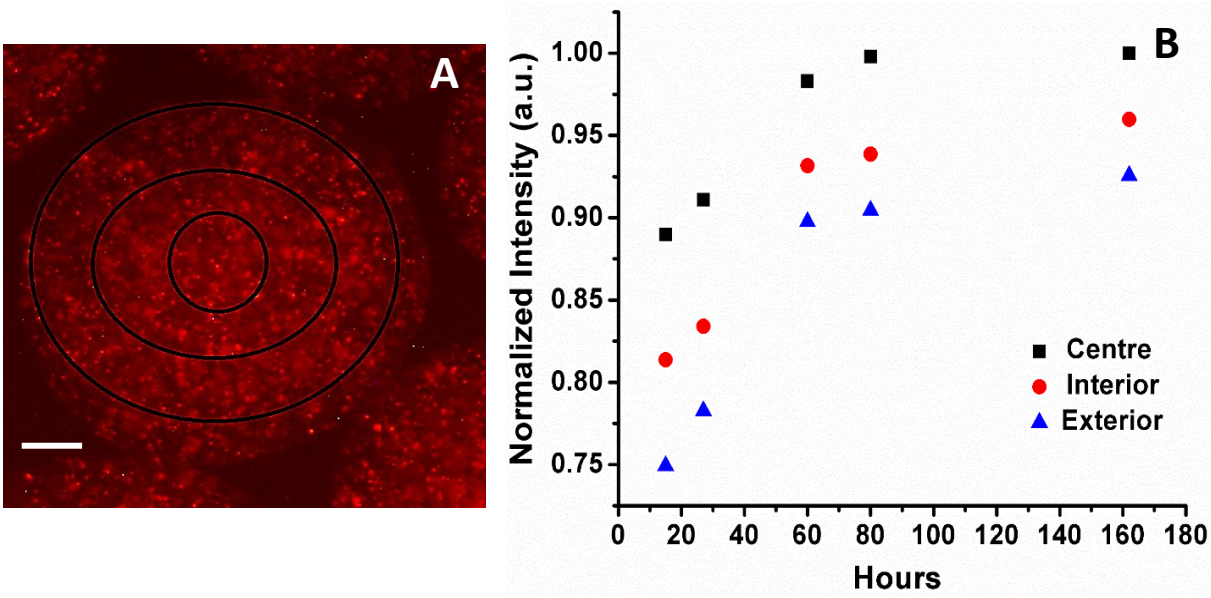

Figure (6A). FNOP distribution in centre, interior and exterior parts [Scale bar-100 µm] (6B). Normalized intensity inside RIN-m5F in one plane of Hydrogel

For Hela cells inside the 3D hydrogel environment, the gradient of oxygen with time (Fig. S4) is approximated with O_2 CaCl2 (mg/L) $= 8.71 * (e^{\left(\frac{-t}{1.93}\right)}) + 3.10$, O_2SrCl2 (mg/L) $= 6.36 * (e^{\left(\frac{-t}{1.32}\right)}) + 2.50$ this showed similar exponential decay but differed in the initial level of oxygen concentration with 2.95 mg/L. As a function of time, the difference in hydrogel oxygen gradient follows a linear curve with a negative slope of 0.68 mg/L.

A confocal image at 84 hours of HeLa cellular hydrogel environment is shown in Fig.7, the plot showed the normalized gradient of oxygen concentration for CaCl2 and SrCl2 gelated hydrogels from the exterior (~0 µm) to centre (~350 µm) of the hydrogel. The gradient followed the sigmoidal curve $A_2 + (A_1 - A_2)/(1 + e^{\left(\frac{x-x_0}{dx}\right)})$ in both the hydrogels, and respective values with standard deviation were shown in Table 1. The strontium gelated hydrogel exhibited a wide range of uniform values and it reached half the value at 295.38± 4.91 µm within the range for the calcium

gelated hydrogel which reached 169.04 ±1.71 μm. A slope of -2.1(a.u. /mm) and -1.5 (a.u. /mm) was observed in SrCl2 and CaCl2 hydrogels. The diffusion coefficient of oxygen in HeLa cells incubated in hydrogel was calculated by using the Fick's law of diffusion equation in considering the rate of time equation and concentration gradient and it was found to be $1.3 * 10^{-9}$ (m^2/sec) which is in the range of the nominal value inside polymeric hydrogels [30-36] . The Oxygen (based on normalized intensity) spatial distribution of CaCl2 and SrCl2 hydrogels without cells (figure S9) demonstrated there was not a large difference in spatial difference in CaCl2 hydrogel with and without cells, while the in SrCl2 (fig.7b) showed the slow decrease of the oxygen gradient inside hydrogels, up to 250 μm from the exterior, which suggested there were more viable cells in SrCl2 compared to CaCl2. This difference is accounted due the reactivity and gel strength with the calcium and strontium ions and is according to the ratio of mannuronic acid (M) and guluronic acid (G) of alginate [37]. The different mechanical strength of extra cellular matrix results in varied behaviour of cancer cell proliferation rate, with higher mechanical strength of extra cellular matrix results in relatively higher proliferation [38]. The current experiments were performed with M/G ratio of 1.56 in alginate, which results in slower gelation rate with strontium when compared to calcium. The decrease in gelation rate exhibit the higher mechanical strength and uniformed structures compared to the faster gelation rate [39, 40]. Calcium and Strontium gelated hydrogel SEM images were shown in (Fig. S8 A and B).

By observing temporal progression and Live and Dead Cell imaging in the hydrogel environment of Insulin cells, we found that the CaCl2 hydrogels showed a viable micro environment compared to SrCl2, whereas for Hela cells on the basis of both temporal and spatial oxygen distribution suggested SrCl2 was a more suitable environment.

In addition to the material suitability to the cellular environment, the application of these highly temporal and spatial resolved monitoring approaches will greatly enhance the design efficiency in producing suitable 3D microenvironments, particularly in additive manufacturing and for different cellular applications.

Table: 1 spatial gradient of Oxygen inside Hydrogel with respect to sigmoidal curve

Hela Cell_3.5 day [$A_2 + (A_1 - A_2)/(1 + e^{(\frac{x-x_0}{dx})})$]				
	CaCl2		SrCl2	
	Value	S.D	Value	S.D
A1	1.02476	0.00457	0.99136	0.002
A2	0.6686	0.00266	0.65026	0.01702
x0	169.04171	1.71293	295.388	4.90776
dx	56.77374	1.83943	40.80	2.978

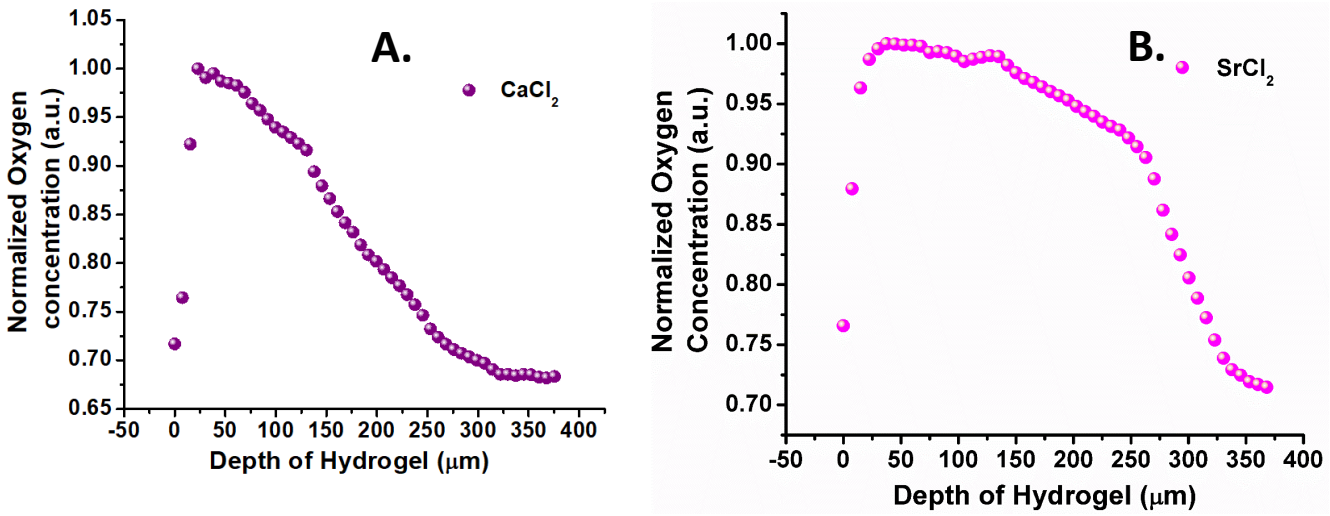

Figure.7 Oxygen gradient in CaCl2 (A) and SrCl2 (B) gelated Hydrogel environment of Hela Cells on 3rd day using confocal microscopy.

Conclusion:

The development of a functional nanoparticle-based oxygen sensor system that can be used to measure the oxygen concentration in 3D hydrogel tissues cultures using fluorescence microscopy has been demonstrated. RIN-m5F, and HeLa cell lines were successfully cultured with FNOPs in calcium and strontium chloride gelation hydrogel environments. In the experiments, the size of the hydrogels generated using an electrospray technique was in the range of 700-1000 μm in diameter. The oxygen concentration gradient tested the cellular viability within the calcium- and strontium-based gelation for RIN-m5F and Hela cells and demonstrated that the two different gelation ions, results in a significant difference in oxygen gradient in 3 Dimensional hydrogel environments and various suitability for different cell types. To address the need to mimic the natural environment, the fabricated FNOP sensor material with the information of high spatial and temporal distribution of oxygen should be extremely valuable in monitoring the 3D tissue material for cellular viability, which will increase the ease and rapid generation of complex and or larger hydrogel structures.

Corresponding Authors

fangang@ess.nthu.edu.tw and j.curran@liverpool.ac.uk

Acknowledgment

We would like to thanks the financial support from MOST, Taiwan by the project: 104-2221-E007-072-MY3, 104-2321-B-007-003, 103-2321-B-007-004, and excellence university centre project for Biomedical Technology, NTHU, and 2013-2016.

References:

(1) Mathers, C. D.; Loncar, D. Projections of global mortality and burden of disease from 2002 to 2030. PLoS medicine 2006, 3, e442.

(2) Mikos, A. G.; Papadaki, M. G.; Kouvroukoglou, S.; Ishaug, S. L.; Thomson, R. C. Mini-review: Islet transplantation to create a bioartificial pancreas. Biotechnol. Bioeng. 1994, 43, 673-677.

(3) Kobayashi, N. Bioartificial pancreas for the treatment of diabetes. Cell Transplant. 2008, 17, 11-17.

(4) Pareta, R. A.; Farney, A. C.; Opara, E. C. Design of a bioartificial pancreas. Pathobiology 2013, 80, 194-202, DOI: 10.1159/000345873 [doi].

(5) Krishnan, R.; Alexander, M.; Robles, L.; Foster, C. E.,3rd; Lakey, J. R. Islet and stem cell encapsulation for clinical transplantation. Rev. Diabet. Stud. 2014, 11, 84-101, DOI: 10.1900/RDS.2014.11.84 [doi].

(6) Lim, F.; Sun, A. M. Microencapsulated islets as bioartificial endocrine pancreas. Science 1980, 210, 908-910.

(7)) Vegas, A. J.; Veiseh, O.; Gürtler, M.; Millman, J. R.; Pagliuca, F. W.; Bader, A. R.; Doloff, J. C.; Li, J.; Chen, M.; Olejnik, K. Long-term glycemic control using polymer-encapsulated human stem cell–derived beta cells in immune-competent mice. Nat. Med. 2016, 22, 306.

(8) Amer, L. D.; Mahoney, M. J.; Bryant, S. J. Tissue engineering approaches to cell-based type 1 diabetes therapy. Tissue Engineering Part B: Reviews 2014, 20, 455-467.

(9) Serra, M.; Brito, C.; Correia, C.; Alves, P. M. Process engineering of human pluripotent stem cells for clinical application. Trends Biotechnol. 2012, 30, 350-359.

(10) Lewis, D. M.; Blatchley, M. R.; Park, K. M.; Gerecht, S. O 2-controllable hydrogels for studying cellular responses to hypoxic gradients in three dimensions in vitro and in vivo. Nature protocols 2017, 12, 1620.

(11) Wang, X.; Wolfbeis, O. S. Optical methods for sensing and imaging oxygen: materials, spectroscopies and applications. Chem. Soc. Rev. 2014, 43, 3666-3761.

(12) Grist, S. M.; Chrostowski, L.; Cheung, K. C. Optical oxygen sensors for applications in microfluidic cell culture. Sensors 2010, 10, 9286-9316.

(13) Hasan, A.; Nurunnabi, M.; Morshed, M.; Paul, A.; Polini, A.; Kuila, T.; Al Hariri, M.; Lee, Y. K.; Jaffa, A. A. Recent advances in application of biosensors in tissue engineering. Biomed. Res. Int. 2014, 2014, 307519, DOI: 10.1155/2014/307519 [doi].

(14) Kautsky, H. Quenching of luminescence by oxygen. Transactions of the Faraday Society 1939, 35, 216-219.

(15) Bergman, I. Rapid-response atmospheric oxygen monitor based on fluorescence quenching. Nature 1968, 218, 396.

(16) Quaranta, M.; Borisov, S. M.; Klimant, I. Indicators for optical oxygen sensors. Bioanalytical reviews 2012, 4, 115-157.

(17) Mills, A. Optical oxygen sensors. Platinum Metals Review 1997, 41, 115-127.

(18) Coogan, M. P.; Gray, V. L.; Hayes, A. J.; Lloyd, S. H.; Millet, C. O.; Pope, S. J.; Lloyd, D. Probing intracellular oxygen by quenched phosphorescence lifetimes of nanoparticles containing polyacrylamide-embedded [Ru (dpp (SO 3 Na) 2) 3] Cl 2. Photochemical & photobiological sciences 2010, 9, 103-109.

(19) Adhikari, B.; Majumdar, S. Polymers in sensor applications. Progress in polymer science 2004, 29, 699-766.

(20) Li, K.; Liu, B. Polymer-encapsulated organic nanoparticles for fluorescence and photoacoustic imaging. Chem. Soc. Rev. 2014, 43, 6570-6597.

(21) Schmälzlin, E.; Van Dongen, J. T.; Klimant, I.; Marmodée, B.; Steup, M.; Fisahn, J.; Geigenberger, P.; Löhmannsröben, H. An optical multifrequency phase-modulation method using microbeads for measuring intracellular oxygen concentrations in plants. Biophys. J. 2005, 89, 1339-1345.

(22) Schmälzlin, E.; Walz, B.; Klimant, I.; Schewe, B.; Löhmannsröben, H. Monitoring hormone-induced oxygen consumption in the salivary glands of the blowfly, Calliphora vicina, by use of luminescent microbeads. Sensors Actuators B: Chem. 2006, 119, 251-254.

(23) Xu, H.; Aylott, J. W.; Kopelman, R. Fluorescent nano-PEBBLE sensors designed for intracellular glucose imaging. Analyst 2002, 127, 1471-1477.

(24) Pedraza, E.; Coronel, M. M.; Fraker, C. A.; Ricordi, C.; Stabler, C. L. Preventing hypoxia-induced cell death in beta cells and islets via hydrolytically activated, oxygen-

generating biomaterials. Proc. Natl. Acad. Sci. U. S. A. 2012, 109, 4245-4250, DOI: 10.1073/pnas.1113560109 [doi].

(25) Benz, K.; Mollenhauer, J. Quality Assessment in 3D Cultures of Disc-Chondrocytes. BioProcess Int 2008, 6.

(26) Yan, Y.; Such, G. K.; Johnston, A. P.; Best, J. P.; Caruso, F. Engineering particles for therapeutic delivery: prospects and challenges. ACS nano 2012, 6, 3663-3669.

(27) Khan, M. I.; Azizli, K.; Sufian, S.; Man, Z.; Khan, A. S. Simultaneous preparation of nano silica and iron oxide from palm oil fuel ash and thermokinetics of template removal. RSC Advances 2015, 5, 20788-20799.

(28) Almería, B.; Gomez, A. Electrospray synthesis of monodisperse polymer particles in a broad (60 nm–2 μm) diameter range: guiding principles and formulation recipes. J. Colloid Interface Sci. 2014, 417, 121-130.

(29) Kim, H. D.; Yi, S. J.; Kim, K. C. Simultaneous measurement of dissolved oxygen concentration and velocity field in microfluidics using oxygen-sensitive particles. Microfluidics and nanofluidics 2013, 15, 139-149.

(30) Kellner, K.; Liebsch, G.; Klimant, I.; Wolfbeis, O. S.; Blunk, T.; Schulz, M. B.; Göpferich, A. Determination of oxygen gradients in engineered tissue using a fluorescent sensor. *Biotechnol. Bioeng.* **2002***, 80*, 73-83.

(31) Lesher-Pérez, S. C.; Kim, G.; Kuo, C.; Leung, B. M.; Mong, S.; Kojima, T.; Moraes, C.; Thouless, M.; Luker, G. D.; Takayama, S. Dispersible oxygen microsensors

map oxygen gradients in three-dimensional cell cultures. *Biomaterials science* **2017***, 5*, 2106-2113.

(32) Malda, J.; Rouwkema, J.; Martens, D. E.; le Comte, E. P.; Kooy, F.; Tramper, J.; van Blitterswijk, C. A.; Riesle, J. Oxygen gradients in tissue-engineered Pegt/Pbt cartilaginous constructs: measurement and modeling. *Biotechnol. Bioeng.* **2004***, 86*, 9-18.

(33) McMurtrey, R. J. Analytic and Numerical Models of Oxygen and Nutrient Diffusion, Metabolism Dynamics, and Architecture Optimization in Three-Dimensional Tissue Constructs with Applications and Insights in Cerebral Organoids.

(34) Super, A.; Jaccard, N.; Marques, M. P. C.; Macown, R. J.; Griffin, L. D.; Veraitch, F. S.; Szita, N. Real-time monitoring of specific oxygen uptake rates of embryonic stem cells in a microfluidic cell culture device. *Biotechnology journal* **2016***, 11*, 1179-1189.

(35) Westphal, I.; Jedelhauser, C.; Liebsch, G.; Wilhelmi, A.; Aszodi, A.; Schieker, M. Oxygen mapping: Probing a novel seeding strategy for bone tissue engineering. *Biotechnol. Bioeng.* **2017***, 114*, 894-902.

(36) Zhao, F.; Pathi, P.; Grayson, W.; Xing, Q.; Locke, B. R.; Ma, T. Effects of oxygen transport on 3-d human mesenchymal stem cell metabolic activity in perfusion and static cultures: Experiments and mathematical model. *Biotechnol. Prog.* **2005**, *21*, 1269-1280.

(37) Mørch, Ý. A.; Donati, I.; Strand, B. L.; Skjåk-Bræk, G. Effect of Ca2 , Ba2 , and Sr2 on alginate microbeads. Biomacromolecules 2006, 7, 1471-1480.

(38) Katira, P.; Bonnecaze, R. T.; Zaman, M. H. Modeling the mechanics of cancer: effect of changes in cellular and extra-cellular mechanical properties. *Frontiers in oncology* **2013**, *3*, 145.

(39) Kaklamani, G.; Cheneler, D.; Grover, L. M.; Adams, M. J.; Bowen, J. Mechanical properties of alginate hydrogels manufactured using external gelation. *Journal of the mechanical behavior of biomedical materials* **2014**, *36*, 135-142.

(40) (2) Kuo, C. K.; Ma, P. X. Ionically crosslinked alginate hydrogels as scaffolds for tissue engineering: Part 1. Structure, gelation rate and mechanical properties. *Biomaterials* **2001**, *22*, 511-521.